ADVANCED FUNCTIONAL MATERIALS
www.afm-journal.de

Check for updates

Hydrogel-Enabled Transfer-Printing of Conducting Polymer Films for Soft Organic Bioelectronics

Shiming Zhang, Haonan Ling, Yihang Chen, Qingyu Cui, Jiahua Ni, Xiaochen Wang, Martin C. Hartel, Xiang Meng, KangJu Lee, Junmin Lee, Wujin Sun, Haisong Lin, Sam Emaminejad, Samad Ahadian, Nureddin Ashammakhi, Mehmet R. Dokmeci, and Ali Khademhosseini**

The use of conducting polymers such as poly(3,4-ethylenedioxythiophene) polystyrene sulfonate (PEDOT:PSS) for the development of soft organic bioelectronic devices, such as organic electrochemical transistors (OECTs), is rapidly increasing. However, directly manipulating conducting polymer thin films on soft substrates remains challenging, which hinders the development of conformable organic bioelectronic devices. A facile transfer-printing of conducting polymer thin films from conventional rigid substrates to flexible substrates offers an alternative solution. In this work, it is reported that PEDOT:PSS thin films on glass substrates, once mixed with surfactants, can be delaminated with hydrogels and thereafter be transferred to soft substrates without any further treatments. The proposed method allows easy, fast, and reliable transferring of patterned PEDOT:PSS thin films from glass substrates onto various soft substrates, facilitating their application in soft organic bioelectronics. By taking advantage of this method, skin-attachable tattoo-OECTs are demonstrated, relevant for conformable, imperceptible, and wearable organic biosensing.

1. Introduction

Since its development in the 1990s, solution-processable conducting polymer poly(3,4-ethylenedioxythiophene) polystyrene sulfonate (PEDOT:PSS) has gained great success due to its high conductivity, optical transparency, as well as stable films properties in both air and water environments.[1–3] These unique properties of PEDOT:PSS have enabled the development of numerous advanced organic electronic devices including solar cells,[4,5] light-emitting diodes,[6] transistors,[7–9] memristors, and artificial synapses for neuromorphic computing.[10–13] Recently, with the rising research trend in flexible electronics,[14–20] which have offered unprecedented opportunities in revolutionizing our understanding of electronic devices,[21–24] PEDOT:PSS

Dr. S. Zhang, Dr. J. Ni, X. Wang, M. C. Hartel, Dr. K. Lee, Dr. J. Lee, Dr. W. Sun, Prof. S. Emaminejad, Dr. S. Ahadian, Prof. N. Ashammakhi, Prof. M. R. Dokmeci, Prof. A. Khademhosseini
Department of Bioengineering
University of California-Los Angeles
Los Angeles, CA 90095, USA
E-mail: shiming.zhang@polymtl.ca; khademh@ucla.edu

Dr. S. Zhang, H. Ling, Y. Chen, Dr. J. Ni, X. Wang, M. C. Hartel, Dr. K. Lee, Dr. J. Lee, Dr. W. Sun, Dr. S. Ahadian, Prof. N. Ashammakhi, Prof. M. R. Dokmeci, Prof. A. Khademhosseini
Center for Minimally Invasive Therapeutics (C-MIT)
University of California-Los Angeles
Los Angeles, CA 90095, USA

Dr. S. Zhang, H. Ling, Y. Chen, Dr. J. Ni, X. Wang, M. C. Hartel, Dr. K. Lee, Dr. J. Lee, Dr. W. Sun, Dr. S. Ahadian, Prof. N. Ashammakhi, Prof. M. R. Dokmeci, Prof. A. Khademhosseini
California NanoSystems Institute
University of California-Los Angeles
Los Angeles, CA 90095, USA

H. Ling
Department of Mechanical and Aerospace Engineering
University of California-Los Angeles
Los Angeles, CA 90095, USA

Y. Chen
Department of Materials Science and Engineering
University of California-Los Angeles
Los Angeles, CA 90095, USA

Dr. Q. Cui
Department of Electrical Engineering and Computer Science
University of Michigan – Ann Arbor
Ann Arbor, MI 48109, USA

Dr. X. Meng
Department of Engineering Physics
Polytechnique Montreal
Montreal, QC H3C 3A7, Canada

H. Lin, Prof. S. Emaminejad
Department of Electrical and Computer Engineering
University of California-Los Angeles
Los Angeles, CA, USA

Prof. N. Ashammakhi, Prof. M. R. Dokmeci, Prof. A. Khademhosseini
Department of Radiology
University of California-Los Angeles
Los Angeles, CA 90095, USA

Prof. A. Khademhosseini
Department of Chemical and Biomolecular Engineering
University of California-Los Angeles
Los Angeles, CA 90095, USA

The ORCID identification number(s) for the author(s) of this article can be found under https://doi.org/10.1002/adfm.201906016.

DOI: 10.1002/adfm.201906016

 © 2019 WILEY-VCH Verlag GmbH & Co. KGaA, Weinheim

16163028, 2020, 6, Downloaded from https://advanced.onlinelibrary.wiley.com/doi/10.1002/adfm.201906016 by The University Of Hong Kong Libraries, Wiley Online Library on [03/01/2026]. See the Terms and Conditions (https://onlinelibrary.wiley.com/terms-and-conditions) on Wiley Online Library for rules of use; OA articles are governed by the applicable Creative Commons License

has extended its important role in developing various flexible organic electronic devices such as organic electrochemical transistors (OECTs),[9,25] an emerging tool for biosensing.[26–37] However, directly manipulating and patterning PEDOT:PSS thin films on flexible substrates remain challenging because of difficulties in obtaining uniform and continuous films on soft substrates such as plastics and elastomers due to their hydrophobic nature.[38] This challenge has been hindering the wide applications of PEDOT:PSS in flexible electronics,[39] particularly for epidermal electronics[40] and conformable OECTs.

Transfer-printing PEDOT:PSS films from glass to flexible substrates offers an alternative solution to circumvent this issue. Thus, several efforts have been dedicated to transfer print PEDOT:PSS onto soft substrates.[38,41,42] Greco et al. proposed a method in which PEDOT:PSS films were deposited on plasma-treated polydimethylsiloxane (PDMS).[41,43] They successfully realized the transfer of PEDOT:PSS ultrathin films to soft substrates by taking advantage of the degradation of adhesion forces between PEDOT:PSS and PDMS over time. Bihar et al. reported PEDOT:PSS application on skin by transferring inkjet-printed PEDOT:PSS films on a tattoo paper.[44] Kim at al.,[45] and Yan et al.[38] have independently demonstrated the transfer-printing of PEDOT:PSS onto flexible substrates by using acid to treat PEDOT:PSS films before the transferring process. Despite these results, each method has certain limitations preventing its versatile application: patterning of PEDOT:PSS films on PDMS suffers from low yield; inkjet printing has limited resolution; and acid treatment involves non-ecofriendly steps which may hinder their use in biological applications.

Here, we present an easy and versatile transfer-printing method to obtain PEDOT:PSS thin films on various soft substrates, encouraging their use in soft organic bioelectronics. These thin films were first processed and patterned on a glass substrate by mixing PEDOT:PSS suspension with surfactants, such as dodecylbenzene sulfonic acid (DBSA). We observed that the addition of surfactant significantly decreased the adhesion forces between PEDOT:PSS films and the glass substrates, which enabled their transfer onto various soft substrates with hydrogel due to the stronger adhesion between PEDOT:PSS and the hydrogel. We discuss in detail how the composition and baking temperature of PEDOT:PSS films affect the efficacy of the transfer. Skin-attachable and ultra-conformable OECTs are finally demonstrated on a tattoo paper by taking advantage of this technique. These skin-attachable OECTs show high performance in terms of sensitivity (transconductance) and ON/OFF ratios, both of which are comparable to their silicon counterparts. In addition, they show stable performance under mechanical deformation on skin. A portable electronic readout system is further developed and integrated with our skin-attachable OECTs, enabling their direct communication with mobile electronic devices. Finally, we demonstrate that our skin-attachable tattoo-OECTs is an ideal platform for monitoring glucose concentrations, relevant for wearable and point-of-care monitoring applications in healthcare.

2. Results and Discussion

The procedure of our transfer-printing method for PEDOT:PSS films is illustrated in **Figure 1**a. Prior to the transfer step, PEDOT:PSS films (doped with DBSA) were spin-coated on glass substrates from suspension (Clevios PH 1000). Thermal annealing may be utilized, depending on the composition of the PEDOT:PSS film (discussed later). Then, a hydrogel carrier (such as agarose, gelatin, and poly(lactic acid) (PVA)) was placed directly on top of the PEDOT:PSS films. Due to the stronger adhesion force between PEDOT:PSS and the hydrogel carrier with respect to that between PEDOT:PSS and glass substrate, detachment of the hydrogel carrier led to a seamless transfer of the PEDOT:PSS films without any residues left on the glass substrate (Video S1, Supporting Information). Next, the hydrogel-carried PEDOT:PSS films were gently placed on target substrates. Pressure was then applied to increase the adhesion at the interface. When water soluble PVA hydrogel carrier was used, the sample was simply immersed in water to dissolve the carrier, thereby finalizing the transfer process onto the target substrate. Significantly, this method proved to be effective in transferring prepatterned PEDOT:PSS films from glass to various soft substrates such as plastics (Figure 1b,c), elastomers (Figure 1d), and human skin (Figure S1, Supporting Information). Given that patterning PEDOT:PSS films on glass can be performed with better established micropatterning technologies compared to soft substrates, this method thus enables facile and rapid patterning of PEDOT:PSS films on soft substrates with high yield.

To gain insight into the dynamic process of our method, we monitored in situ resistance changes of the PEDOT:PSS film during hydrogel stamp removal. We first bridged the PEDOT:PSS-attached hydrogel carrier between pre-patterned Au electrodes on glass. The sample was then immersed in water to dissolve the hydrogel carrier. As shown in **Figure 2**a, upon water immersion, the resistivity between the electrodes gradually decreased and reached its lowest value after 2 min, demonstrating the completion of the transfer process. A high conductivity of 400 S cm^{-1} was calculated for PEDOT:PSS films transferred on the target substrates (Figure 2b), which was comparable to those values on glass.[46] The conductivity showed a slight decrease after water immersion (Figure 2c), which was likely due to water absorption by the hydrophilic PSS^- chains, similar to films deposited on glass substrates.[47]

Secondary-dopants are often used to tune the conductivity, flexibility, and adhesion forces of PEDOT:PSS thin films.[2,47,48] Evaluating the efficacy of our transfer-printing method for films of different compositions is essential towards ensuring its versatile use. We investigated the feasibility of transfer-printing PEDOT:PSS films processed with different secondary-dopants, including DBSA, conductivity enhancer glycerol, plasticizer Capstone FS-30, and crosslinker glycidoxypropyltrimethoxysilane (GOPS). We simultaneously investigated the effects of annealing on the transfer-printing process. For the annealing process, films were baked at 120 °C for different times ranging from 10 s to 30 min. Figure 2d summarizes the effect of different compositions of PEDOT:PSS and annealing times on the transfer-printing. Figure 2e shows the chemical structures of the various additives used in this study. We summarized these results as follows: (i) longer baking time increases adhesion between PEDOT:PSS and glass and thus is not preferable for transfer-printing; (ii) the presence of DBSA in the films promotes transfer-printing process; and (iii) addition of the crosslinker into PEDOT:PSS hinders the transfer-printing. For example, the pristine PEDOT:PSS could be transferred onto

© 2019 WILEY-VCH Verlag GmbH & Co. KGaA, Weinheim

16163028, 2020, 6, Downloaded from https://advanced.onlinelibrary.wiley.com/doi/10.1002/adfm.201906016 by The University Of Hong Kong Libraries, Wiley Online Library on [03/01/2026]. See the Terms and Conditions (https://onlinelibrary.wiley.com/terms-and-conditions) on Wiley Online Library for rules of use; OA articles are governed by the applicable Creative Commons License

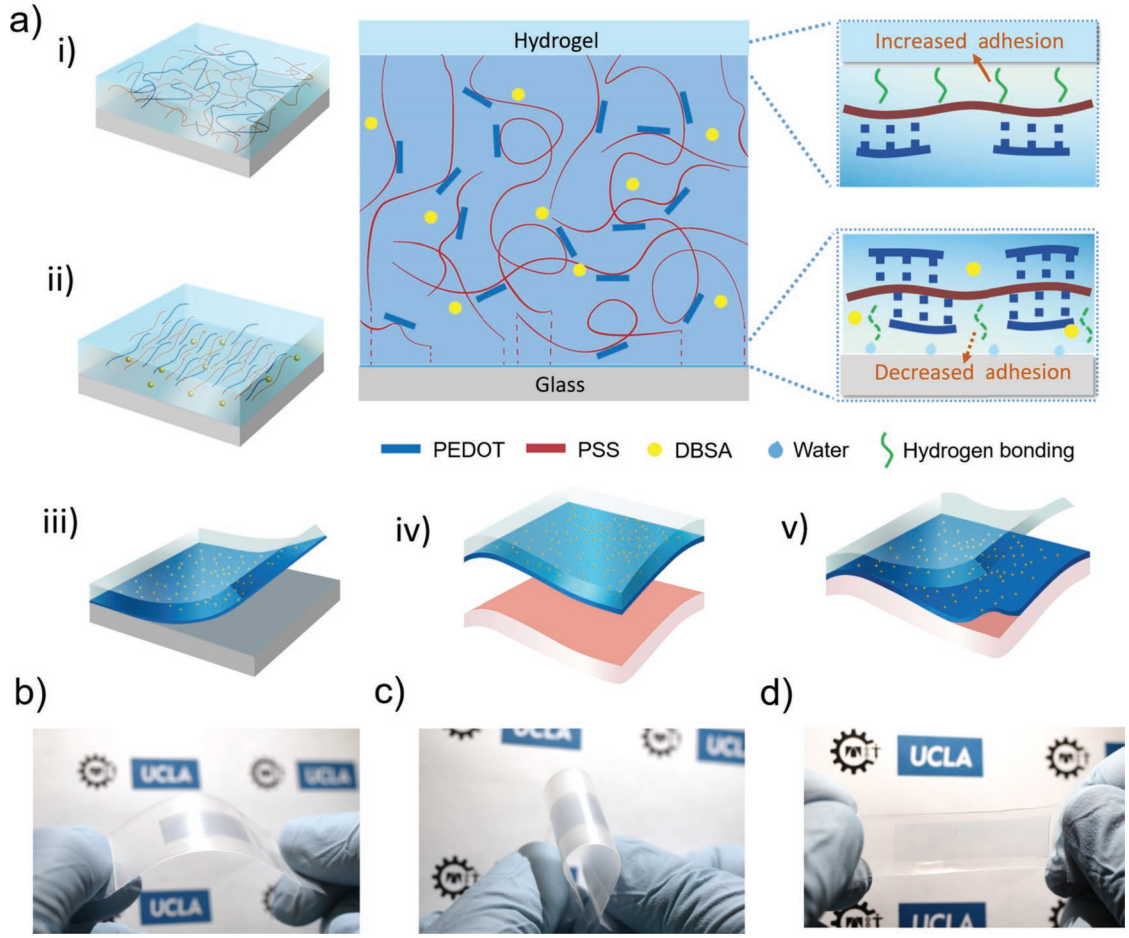

Figure 1. Transfer-printing procedure of PEDOT:PSS films (5 v/v% glycerol and 1 v/v% DBSA). a) Schematic image of the procedure for the transfer-printing of DBSA-treated PEDOT:PSS films onto target substrates: (i) Spin-coating PEDOT:PSS on glass substrates; (ii) Baking the PEDOT:PSS (w/ DBSA) on glass; (iii) PEDOT:PSS film peeling-off with hydrogel; (iv) laminating the PEDOT:PSS/hydrogel onto target soft substrates; (v) Removal of the hydrogel carrier finalized the transfer of PEDOT:PSS films onto target substrates. Zoomed in diagram hypothesized an increased hydrogen-bonding between PEDOT:PSS and hydrogel (green), and decreased adhesion force between DBSA-treated PEDOT:PSS and glass (dotted green); b,c) flexible PEDOT:PSS films transferred onto plastic; and d) stretchable PEDOT:PSS film transferred onto PDMS.

the hydrogel before baking was performed, but failure occurred immediately after baking for 30 s. Significantly, after adding DBSA, films could be successfully transferred even after baking for 30 min, as long as GOPS was not presented, suggesting the effectiveness of DBSA in facilitating the peeling-off of PEDOT:PSS from donor substrates (Figure S2, Supporting Information). These exciting results point to a key contribution of this work: the combination of DBSA-doped PEDOT:PSS and hydrogel stamps enables the efficient transfer-printing of PEDOT:PSS films without the use of any other chemicals or complicated surface treatments. Our approach is therefore superior to other transfer-printing methods that rely on hydrophobic interfaces, acid treatments, or strong oxidants (Summarized in **Table 1**).

The mechanism of our method in transfer-printing PEDOT:PSS films is tentatively attributed to the hydrogen bonding between the hydrogel and PSS (which contains hydrophilic SO_3^- groups), as well as decreased adhesion between PEDOT:PSS and glass substrates due to the addition of DBSA. The hydrogel contains a large amount of water, which, upon contact with PEDOT:PSS, induces swelling of PEDOT:PSS films (Figure S3, Supporting Information) and eases the formation of hydrogen bonding with PSS at the interface. This was further confirmed by comparison experiments in which conventional PDMS carriers (w/ or w/o plasma treatment) failed to peel-off films from glass (Video S2, Supporting Information), demonstrating their weaker adhesion forces compared to those between PEDOT:PSS and the hydrogel. To clarify the role of DBSA in decreasing the adhesion between PEDOT:PSS and glass, we conducted a peeling experiment where all samples were stretched at a constant rate using a tensile tester (**Figure 3**a). We observed that samples with DBSA were delaminated easily from the glass substrate to the hydrogel, while failures occurred in all reference samples without DBSA (Figure 3b). Meanwhile, a much lower adhesion force with glass was measured for films with DBSA (Figure 3c). This is because DBSA is a surfactant (wettability enhancer) whose molecules contain hydrophilic SO_3^- tails, which can significantly increase the water affinity of the resultant PEDOT:PSS films. This increase could be visualized by the lower contact angles recorded for films containing DBSA (Figure 3d). Furthermore, we surmise

 © 2019 WILEY-VCH Verlag GmbH & Co. KGaA, Weinheim

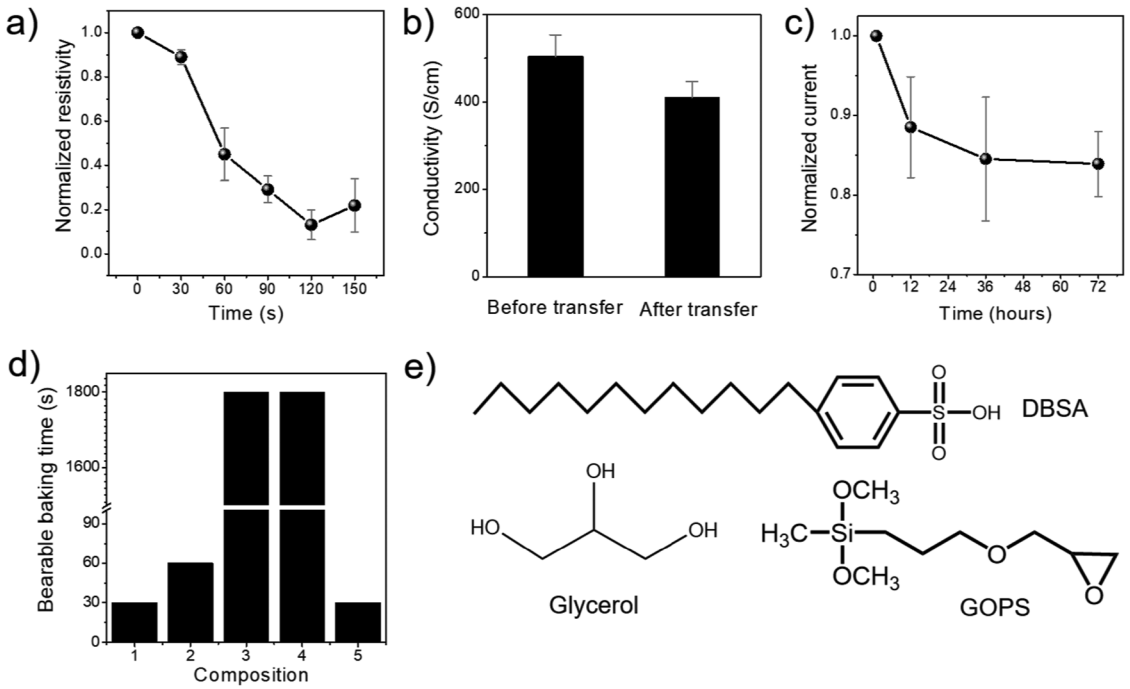

Figure 2. a) Dynamic resistivity change during transfer-printing of PEDOT:PSS films from glass onto a plastic PET substrate; b) Conductivity comparison of PEDOT:PSS film (5 v/v% glycerol and 1 v/v% DBSA) before and after transfer; c) Water stability of transferred PEDOT:PSS films on plastic; d) Maximum baking time after which film delamination failure occurs. The numbers in the x axis refer to PEDOT:PSS with difference compositions: (1) pristine PEDOT:PSS; (2) PEDOT:PSS: 5 v/v% glycerol; (3) PEDOT:PSS: 1 v/v% DBSA; (4) PEDOT:PSS: 1 v/v% Capstone; (5) PEDOT:PSS: 1 v/v% DBSA: 1 v/v% GOPS. The baking temperature was 120 °C; e) Chemical structures of additives used in processing PEDOT:PSS films: DBSA, conductivity enhancer glycerol, and crosslinker GOPS.

that DBSA molecules can facilitate water diffusion from the hydrogel to PEDOT:PSS porous networks and their further migration to the underlying glass substrate. Such migration leads to the formation of a water boundary layer that decreases adhesion at the PEODT:PSS–glass interface. According to the tentative transfer-printing mechanism discussed above, other surfactants which increase the film wettability should also enable the PEDOT:PSS films to be peeled off with a hydrogel carrier. To verify this assumption, we used Capstone FS-30, a fluorinated surfactant with similar functionality as compared to DBSA. In line with our expectations, films doped with capstone FS-30 were successfully peeled-off using hydrogel, demonstrating that the presence of surfactants is essential to decrease the adhesion between PEDOT:PSS and glass, thereby enabling the transfer-printing process.

Using our transfer-printing method, we were able to develop functional flexible electronic devices based on PEDOT:PSS. Specifically, it allowed us to develop skin-attachable OECTs on tattoo paper (**Figure 4**) which could subsequently be transferred onto human skin (Figure S4 and Video S3, Supporting Information). We demonstrated skin-attachable OECTs by first depositing and patterning source and drain electrodes on a commercially available tattoo paper with a laser-ablated shadow mask, followed by transfer-printing patterned PEDOT:PSS thin films (with 5 v/v% glycerol and 0.5 v/v% DBSA) in between the electrodes (Figure 4a). The obtained OECTs could be laminated directly onto the skin by dissolving the supporting substrate of the tattoo paper with water (Video S4, Supporting Information). Significantly, our skin-attachable OECTs showed ultraconformable contact with skin (Figure 4b; Video S5, Supporting Information) and no delamination was observed even upon flushing with water (Video S6, Supporting Information), suggesting its robust adhesion on soft substrates and the potential for long-term use.

Table 1. Comparison of various transfer-printing technologies for PEDOT:PSS films.

References	Donor substrates	Required treatment	Carrier	Required post-treatment
[41,43]	PDMS	O_2 plasma	PVA	Not needed
[42]	Glass	Ethanol dropping	Plastic plymethylpentene	Ethanol dropping
[45]	Glass	H_2SO_4 immersion	PDMS	Annealing needed
[38]	Glass	CH_4SO_3/H_3PO_4 immersion	PDMS	Annealing needed
This work	Glass/Plastic/PDMS	Not needed	Hydrogel	Not needed

© 2019 WILEY-VCH Verlag GmbH & Co. KGaA, Weinheim

16163028, 2020, 6, Downloaded from https://advanced.onlinelibrary.wiley.com/doi/10.1002/adfm.201906016 by The University Of Hong Kong Libraries, Wiley Online Library on [03/01/2026]. See the Terms and Conditions (https://onlinelibrary.wiley.com/terms-and-conditions) on Wiley Online Library for rules of use; OA articles are governed by the applicable Creative Commons License

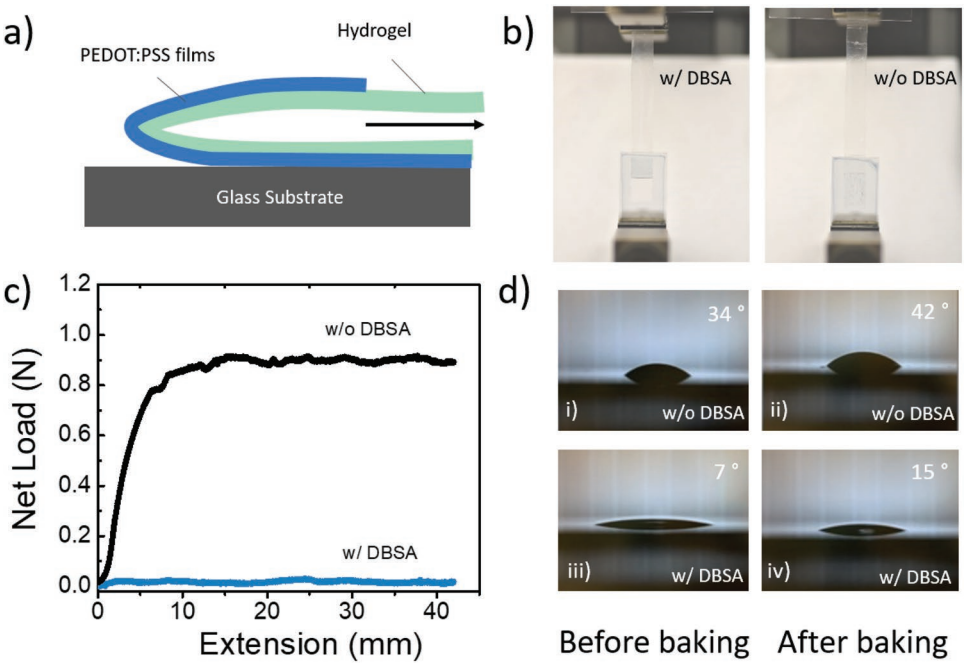

Figure 3. a) Schematic illustration of the process for the peeling test; b) PEDOT:PSS films with addition of 1v/v% DBSA were successfully peeled-off from glass substrates with a PVA hydrogel carrier while the reference samples (w/o DBSA) failed to be peeled-off; c) Net load comparison during the delamination test, both samples were stretched at the same speed of 0.1 mm s^{-1}; d) Contact-angle comparison of films w/ and w/o DBSA addition, before and after baking for 30 min (120 °C).

The transient plots of the OECTs with transfer-printed PEDOT:PSS films showed stable baseline after cyclic measurements (Figure S5, Supporting Information). From the transient plot, we extracted a decay constant of ≈300 ms, which can be attributed to the relatively large dimension of the device (W of 10 mm, L of 1 mm). The output and transfer characteristics of the OECTs showed typical behavior for PEDOT:PSS OECTs working in depletion mode (Figure 4c,d). From the transfer curves (i.e., source–drain current (I_{ds}) sensitivity to gate voltage (V_{gs}) variations), we extracted a maximum transconductance of about 1.5 mS (V_{gs} = 0 V), and an ON/OFF ratio of ≈50 (I_{ds} (V_{gs} = 0 V)/I_{ds} (V_{gs} = 0.8 V)). It is noteworthy that during mechanical deformation of the skin (e.g., stretching and compressing), the electrical characteristics of the devices remained relatively stable (Figure 4c–e), indicating their potential for future wearable biosensing applications.

In order to demonstrate the promise of our skin-attachable OECTs for wearable biosensing applications, we further developed a data readout system with wireless communication capabilities. The system was built to be as compact as possible (Figure S6, Supporting Information) for better portability. It is composed of a micro-controller unit (MCU, Arduino) with an analog to digital converter (ADC) and a Bluetooth communication (Simblee), an independent power supply based on button batteries, a digital to analog converter (DAC) modules, variable reference resistors and the corresponding peripheral wirings, as shown in the **Figure 5**a,b. The source of the OECT was grounded and the drain was connected to a reference resistance, which was wired to the battery. The ADC input was employed to monitor the voltage of the drain terminal, and the converted data was collected and processed in the MCU. The waveform of the acquired data represented the timing variation sequence of the channel current going through the OECT. Meanwhile, the MCU also generated signals to control the DAC, which was connected to the gate of the OECT with the voltage down to the scale of millivolt. Finally, the data was transmitted out by the Bluetooth module embedded in the MCU to an external mobile device where the data was shown and interfaced with customized APPs for real-time monitoring.

Our skin-attachable OECTs on tattoo paper serve as a versatile platform for soft organic bioelectronics. As a prototype, we demonstrate the use of tattoo-OECTs for the detection of glucose, which is a health indicator in screening metabolic diseases such as diabetics.[21] For the glucose sensor, the enzyme (GO_x) was deposited on a platinum (Pt)[49–51] gate electrode. The sensing mechanism is described in previous works[50,51] where GO_x catalyzes the conversion of D-glucose to D-gluconо-1,5-lactone, and becomes reduced. Oxygen molecules in the electrolyte then react with reduced GO_x to form hydrogen peroxide. The Pt gate catalyzes the decomposition of peroxide, finally leading to an electrochemical reaction at the electrodes (Figure 5c,d). The effective gate voltage and the variation of I_{ds} are thus related to the concentration of the glucose in the electrolyte. Figure 5e,f shows the response of our OECTs to various glucose concentrations. The I_{ds} showed a monotonic decrease with increasing glucose concentrations up to 0.1 M, with the ability to detect glucose concentrations as low as 1×10^{-6} M, demonstrating the potential of our tattoo-OECTs as conformable, ultralightweight, and noninvasive biosensor for future personalized healthcare applications.

© 2019 WILEY-VCH Verlag GmbH & Co. KGaA, Weinheim

16163028, 2020, 6, Downloaded from https://advanced.onlinelibrary.wiley.com/doi/10.1002/adfm.201906016 by The University Of Hong Kong Libraries, Wiley Online Library on [03/01/2026]. See the Terms and Conditions (https://onlinelibrary.wiley.com/terms-and-conditions) on Wiley Online Library for rules of use; OA articles are governed by the applicable Creative Commons License

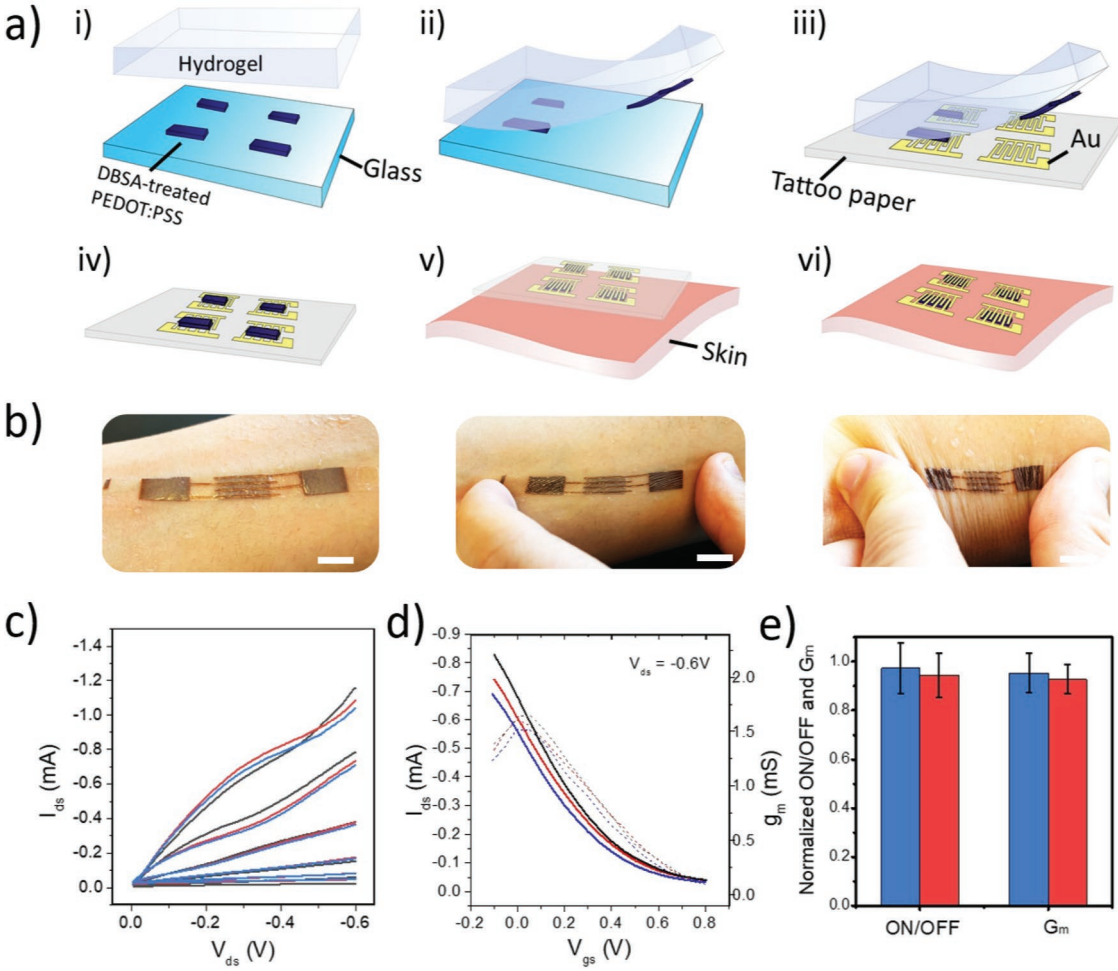

Figure 4. a) Schematic illustration of the generic process for transfer-printing DBSA-treated PEDOT:PSS films with hydrogel: (i) laminating a hydrogel stamp against glass donor substrate; (ii) gently peeling-off the stamp leads to the transfer of patterned PEDOT:PSS films from the glass substrate onto the hydrogel stamp; (iii) laminating the stamp onto target tattoo paper; and (iv) dissolving the hydrogel stamp transfers the patterned PEDOT:PSS films to the tattoo paper; (v) laminating the tattoo paper onto skin. Tattoo adhesive tapes were used only at the edges to increase adhesion between tattoo and skin by exposing the PEDOT:PSS channel directly to skin. The PEDOT:PSS films adhered well to skin via Van der Waals force due to its ultrathin thickness; (vi) dissolving the tattoo paper with water transferred the OECTs onto skin. b) Optical images of the skin-attachable OECTs under mechanical deformation. The scale bar is 6 mm; c,d) Output (V_{gs}: −0.2 to 0.8 V) and transfer curves (V_{ds} = −0.6 V) of skin-attachable OECTs at released (red), 5% stretched (blue) and 40% compressed (black) conditions; The width (W) of the channel is 10 mm, the length (L) of the channel is 1 mm (W/L = 10); e) ON/OFF and transconductance (G_m) comparison of skin-attachable OECTs before and after compressed for ten times.

3. Conclusion

In conclusion, we have demonstrated that PEDOT:PSS films on glass, upon being mixed with surfactants such as DBSA, can be easily delaminated with hydrogel carriers. By taking advantage of this phenomenon, we have developed a simple, fast, ecofriendly, and versatile transfer-printing technique that allows the transfer of PEDOT:PSS films onto various soft substrates. This method can easily be tailored to obtain patterned PEDOT:PSS films on flexible substrates, encouraging its wide application in flexible electronics. Mechanism of the successful transfer of PEDOT:PSS films onto the hydrogel was attributed to reduced adhesion between PEDOT:PSS and glass due to the addition of DBSA. By taking advantage of this method, along with the integration of a miniaturized wireless readout system, we have developed skin-attachable OECTs on tattoo paper, relevant for ultralightweight, conformable, and wearable biosensing.

Our approach provides an advanced technological platform to fabricate flexile organic electronics based on PEDOT:PSS thin films. In addition, it may also be applicable to pattern other conducting polymers. This work thus paves the way for developing next-generation soft organic electronic and bioelectronic devices towards wearable healthcare monitoring applications.

Supporting Information

Supporting Information is available from the Wiley Online Library or from the author.

© 2019 WILEY-VCH Verlag GmbH & Co. KGaA, Weinheim

16163028, 2020, 6, Downloaded from https://advanced.onlinelibrary.wiley.com/doi/10.1002/adfm.201906016 by The University Of Hong Kong Libraries, Wiley Online Library on [03/01/2026]. See the Terms and Conditions (https://onlinelibrary.wiley.com/terms-and-conditions) on Wiley Online Library for rules of use; OA articles are governed by the applicable Creative Commons License

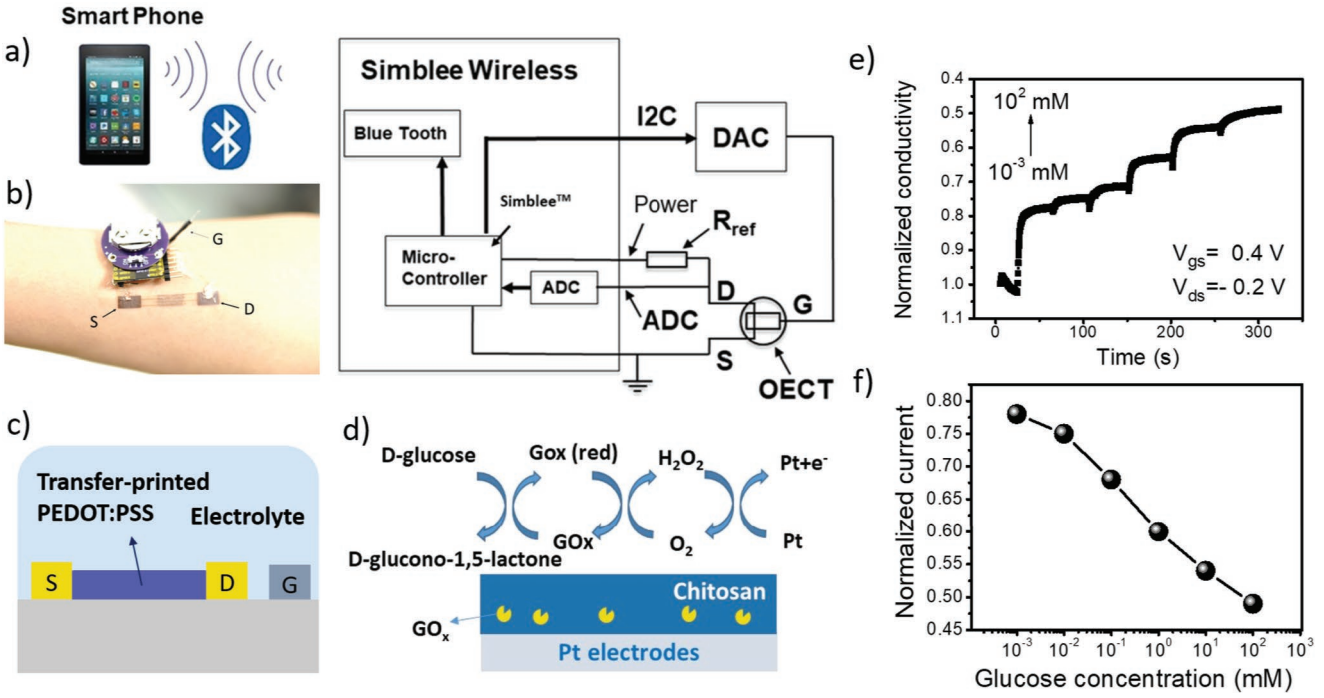

Figure 5. a) Block diagram of the interface circuit for wireless electrical performance characterization of the skin-attachable OECTs; b) Optical image of the integration of OECTs with wireless readout system; c) Schematic illustration of the structure of OECTs; d) Modification of the platinum gate electrodes (G) in c) with GO_x and chitosan, and the biocatalyzed reaction cycle involved in the detection of glucose using GO_x; e) Transient I_{ds} response to different concentrations of glucose in PBS; and f) Normalized I_{ds} with respect to different glucose concentrations.

Acknowledgements

S.Z. and H.L. contributed equally to this work. The authors are grateful to Prof. Alberto Salleo at Department of Materials Science and Engineering, Stanford University, for fruitful discussions. The authors also acknowledge the user facilities UCLA Nanoelectronics Research Facility (NRF) and Integrated Systems Nanofabrication Cleanroom (ISNC) in California NanoSystems Institute (CNSI). The authors would like to thank NRF staff member Hoc Quang Ngo, and ISNC staff members Tony Wright, Lorna Tokunaga, and Krissy Do for invaluable insight and support during this study. This work has been supported by the National Institutes of Health (1R01HL140951-01A1, 1R01GM126571-01, 1R01GM126831-01, 1R01EB023052-01A1). For all demonstrations on human skin, a signed consent was obtained from the volunteer.

Conflict of Interest

The authors declare no conflict of interest.

Keywords

hydrogel, OECTs, PEDOT:PSS, transfer-printing, wearable biosensing

Received: July 24, 2019
Revised: October 3, 2019
Published online: November 22, 2019

[1] L. Groenendaal, F. Jonas, D. Freitag, H. Pielartzik, J. R. Reynolds, *Adv. Mater.* **2000**, *12*, 481.
[2] Y. Wang, C. Zhu, R. Pfattner, H. Yan, L. Jin, S. Chen, F. Molina-Lopez, F. Lissel, J. Liu, N. I. Rabiah, Z. Chen, J. W. Chung, C. Linder, M. F. Toney, B. Murmann, Z. Bao, *Sci. Adv.* **2017**, *3*, e1602076.
[3] L. V. Kayser, D. J. Lipomi, *Adv. Mater.* **2019**, *31*, 1806133.
[4] Y. H. Kim, C. Sachse, M. L. Machala, C. May, L. Müller-Meskamp, K. Leo, *Adv. Funct. Mater.* **2011**, *21*, 1076.
[5] D. J. Lipomi, B. C.-K. Tee, M. Vosgueritchian, Z. Bao, *Adv. Mater.* **2011**, *23*, 1771.
[6] Y.-s. Liu, J. Feng, X.-L. Ou, H.-f. Cui, M. Xu, H.-B. Sun, *Org. Electron.* **2016**, *31*, 247.
[7] S. Inal, G. G. Malliaras, J. Rivnay, *Nat. Commun.* **2017**, *8*, 1767.
[8] D. Khodagholy, J. Rivnay, M. Sessolo, M. Gurfinkel, P. Leleux, L. H. Jimison, E. Stavrinidou, T. Herve, S. Sanaur, R. M. Owens, G. G. Malliaras, *Nat. Commun.* **2013**, *4*, 2133.
[9] J. Rivnay, S. Inal, A. Salleo, R. M. Owens, M. Berggren, G. G. Malliaras, *Nat. Rev. Mater.* **2018**, *3*, 17086.
[10] Y. van de Burgt, A. Melianas, S. T. Keene, G. Malliaras, A. Salleo, *Nat. Electron.* **2018**, *1*, 386.
[11] Y. van de Burgt, E. Lubberman, E. J. Fuller, S. T. Keene, G. C. Faria, S. Agarwal, M. J. Marinella, A. Alec Talin, A. Salleo, *Nat. Mater.* **2017**, *16*, 414.
[12] P. Gkoupidenis, N. Schaefer, B. Garlan, G. G. Malliaras, *Adv. Mater.* **2015**, *27*, 7176.
[13] P. Gkoupidenis, N. Schaefer, X. Strakosas, J. A. Fairfield, G. G. Malliaras, *Appl. Phys. Lett.* **2015**, *107*, 263302.
[14] T.-G. La, S. Qiu, D. K. Scott, R. Bakhtiari, J. W. P. Kuziek, K. E. Mathewson, J. Rieger, H.-J. Chung, *Adv. Healthcare Mater.* **2018**, *7*, 1801033.
[15] A. Kumar, H. Saghlatoon, T.-G. La, M. Mahdi Honari, H. Charaya, H. Abu Damis, R. Mirzavand, P. Mousavi, H.-J. Chung, *Flexible Printed Electron.* **2017**, *2*, 045001.
[16] T. Kim, C. Bao, M. Hausmann, G. Siqueira, T. Zimmermann, W. S. Kim, *Adv. Electron. Mater.* **2019**, *5*, 1800778.

© 2019 WILEY-VCH Verlag GmbH & Co. KGaA, Weinheim

16163028, 2020, 6, Downloaded from https://advanced.onlinelibrary.wiley.com/doi/10.1002/adfm.201906016 by The University Of Hong Kong Libraries, Wiley Online Library on [03/01/2026]. See the Terms and Conditions (https://onlinelibrary.wiley.com/terms-and-conditions) on Wiley Online Library for rules of use; OA articles are governed by the applicable Creative Commons License

[17] A. J. Hackett, J. Malmström, J. Travas-Sejdic, *ACS Appl. Energy Mater.* **2019**, *2*, 1436.
[18] P. Baek, L. Voorhaar, D. Barker, J. Travas-Sejdic, *Acc. Chem. Res.* **2018**, *51*, 1581.
[19] C. Wang, C. Wang, Z. Huang, S. Xu, *Adv. Mater.* **2018**, *30*, 1801368.
[20] A. Servati, L. Zou, Z. J. Wang, F. Ko, P. Servati, *Sensors* **2017**, *17*, 1622.
[21] W. Gao, S. Emaminejad, H. Y. Y. Nyein, S. Challa, K. Chen, A. Peck, H. M. Fahad, H. Ota, H. Shiraki, D. Kiriya, D.-H. Lien, G. A. Brooks, R. W. Davis, A. Javey, *Nature* **2016**, *529*, 509.
[22] C. Wang, X. Li, H. Hu, L. Zhang, Z. Huang, M. Lin, Z. Zhang, Z. Yin, B. Huang, H. Gong, S. Bhaskaran, Y. Gu, M. Makihata, Y. Guo, Y. Lei, Y. Chen, C. Wang, Y. Li, T. Zhang, Z. Chen, A. P. Pisano, L. Zhang, Q. Zhou, S. Xu, *Nat. Biomed. Eng.* **2018**, *2*, 687.
[23] Z. Huang, Y. Hao, Y. Li, H. Hu, C. Wang, A. Nomoto, T. Pan, Y. Gu, Y. Chen, T. Zhang, W. Li, Y. Lei, N. Kim, C. Wang, L. Zhang, J. W. Ward, A. Maralani, X. Li, M. F. Durstock, A. Pisano, Y. Lin, S. Xu, *Nat. Electron.* **2018**, *1*, 473.
[24] K. Sim, Z. Rao, H.-J. Kim, A. Thukral, H. Shim, C. Yu, *Sci. Adv.* **2019**, *5*, eaav5749.
[25] S. Zhang, E. Hubis, G. Tomasello, G. Soliveri, P. Kumar, F. Cicoira, *Chem. Mater.* **2017**, *29*, 3126.
[26] S. Inal, J. Rivnay, A.-O. Suiu, G. G. Malliaras, I. McCulloch, *Acc. Chem. Res.* **2018**, *51*, 1368.
[27] D. Khodagholy, T. Doublet, P. Quilichini, M. Gurfinkel, P. Leleux, A. Ghestem, E. Ismailova, T. Hervé, S. Sanaur, C. Bernard, G. G. Malliaras, *Nat. Commun.* **2013**, *4*, 1575.
[28] M. Berggren, A. Richter-Dahlfors, *Adv. Mater.* **2007**, *19*, 3201.
[29] D. T. Simon, E. O. Gabrielsson, K. Tybrandt, M. Berggren, *Chem. Rev.* **2016**, *116*, 13009.
[30] C. Liao, C. Mak, M. Zhang, H. L. W. Chan, F. Yan, *Adv. Mater.* **2015**, *27*, 676.
[31] Y. Fu, N. Wang, A. Yang, H. K.-w. Law, L. Li, F. Yan, *Adv. Mater.* **2017**, *29*, 1703787.
[32] A. Yang, Y. Li, C. Yang, Y. Fu, N. Wang, L. Li, F. Yan, *Adv. Mater.* **2018**, *30*, 1800051.
[33] O. Parlak, S. T. Keene, A. Marais, V. F. Curto, A. Salleo, *Sci. Adv.* **2018**, *4*, eaar2904.
[34] S. Zhang, F. Cicoira, *Nature* **2018**, *561*, 466.
[35] N. Saraf, E. R. Woods, M. Peppler, S. Seal, *Biosens. Bioelectron.* **2018**, *117*, 40.
[36] S. Wustoni, S. Wang, J. R. Alvarez, T. C. Hidalgo, S. P. Nunes, S. Inal, *Biosens. Bioelectron.* **2019**, *143*, 111561.
[37] Y. Liang, C. Wu, G. Figueroa-Miranda, A. Offenhäusser, D. Mayer, *Biosens. Bioelectron.* **2019**, *144*, 111668.
[38] X. Fan, B. Xu, S. Liu, C. Cui, J. Wang, F. Yan, *ACS Appl. Mater. Interfaces* **2016**, *8*, 14029.
[39] T. Sekitani, T. Someya, *Adv. Mater.* **2010**, *22*, 2228.
[40] D.-H. Kim, N. Lu, R. Ma, Y.-S. Kim, R.-H. Kim, S. Wang, J. Wu, S. M. Won, H. Tao, A. Islam, K. J. Yu, T.-i. Kim, R. Chowdhury, M. Ying, L. Xu, M. Li, H.-J. Chung, H. Keum, M. McCormick, P. Liu, Y.-W. Zhang, F. G. Omenetto, Y. Huang, T. Coleman, J. A. Rogers, *Science* **2011**, *333*, 838.
[41] F. Greco, A. Zucca, S. Taccola, B. Mazzolai, V. Mattoli, *ACS Appl. Mater. Interfaces* **2013**, *5*, 9461.
[42] L. Yin, Z. Zhao, F. Jiang, Z. Li, S. Xiong, Y. Zhou, *Org. Electron.* **2014**, *15*, 2593.
[43] F. Greco, A. Zucca, S. Taccola, A. Menciassi, T. Fujie, H. Haniuda, S. Takeoka, P. Dario, V. Mattoli, *Soft Matter* **2011**, *7*, 10642.
[44] E. Bihar, T. Roberts, Y. Zhang, E. Ismailova, T. Hervé, G. G. Malliaras, J. B. De Graaf, S. Inal, M. Saadaoui, *Flexible Printed Electron.* **2018**, *3*, 034004.
[45] N. Kim, H. Kang, J.-H. Lee, S. Kee, S. H. Lee, K. Lee, *Adv. Mater.* **2015**, *27*, 2317.
[46] P. Kumar, Z. Yi, S. Zhang, A. Sekar, F. Soavi, F. Cicoira, *Appl. Phys. Lett.* **2015**, *107*, 053303.
[47] S. Zhang, P. Kumar, A. S. Nouas, L. Fontaine, H. Tang, F. Cicoira, *APL Mater.* **2015**, *3*, 014911.
[48] S. Savagatrup, E. Chan, S. M. Renteria-Garcia, A. D. Printz, A. V. Zaretski, T. F. O'Connor, D. Rodriquez, E. Valle, D. J. Lipomi, *Adv. Funct. Mater.* **2015**, *25*, 427.
[49] H. Tang, F. Yan, P. Lin, J. Xu, H. L. W. Chan, *Adv. Funct. Mater.* **2011**, *21*, 2264.
[50] D. A. Bernards, D. J. Macaya, M. Nikolou, J. A. DeFranco, S. Takamatsu, G. G. Malliaras, *J. Mater. Chem.* **2008**, *18*, 116.
[51] D. J. Macaya, M. Nikolou, S. Takamatsu, J. T. Mabeck, R. M. Owens, G. G. Malliaras, *Sens. Actuators, B* **2007**, *123*, 374.

© 2019 WILEY-VCH Verlag GmbH & Co. KGaA, Weinheim

16163028, 2020, 6, Downloaded from https://advanced.onlinelibrary.wiley.com/doi/10.1002/adfm.201906016 by The University Of Hong Kong Libraries, Wiley Online Library on [03/01/2026]. See the Terms and Conditions (https://onlinelibrary.wiley.com/terms-and-conditions) on Wiley Online Library for rules of use; OA articles are governed by the applicable Creative Commons License